Cancer Management and Research

Elevate Series

Open Access Full Text Article

ORIGINAL RESEARCH

Development and Cross-Institutional Validation of a Comprehensive Machine Learning Model Predicting Response to Neoadjuvant Therapy for Rectal Cancer

Sha Li[1,2], Zhengxian Li[3], Shuai Li[2], Ping Jiang[4], Hongbin Han[1], Yibao Zhang[2], Yanye Lu[1,5]

[1]Institute of Medical Technology, Peking University Health Science Center, Peking University, Beijing, People's Republic of China; [2]Key Laboratory of Carcinogenesis and Translational Research (Ministry of Education / Beijing), Department of Radiation Oncology, Peking University Cancer Hospital & Institute, Beijing Cancer Hospital & Institute, Beijing, People's Republic of China; [3]Department of Radiotherapy, Guowen Hospital, Jilin, People's Republic of China; [4]Department of Radiation Oncology, Peking University Third Hospital, Beijing, People's Republic of China; [5]National Biomedical Imaging Center, Peking University, Beijing, People's Republic of China

Correspondence: Yibao Zhang, Key Laboratory of Carcinogenesis and Translational Research (Ministry of Education / Beijing), Department of Radiation Oncology, Peking University Cancer Hospital & Institute, Beijing Cancer Hospital & Institute, Beijing, People's Republic of China, Email zhangyibao@pku.edu.cn; Yanye Lu, Email yanye.lu@pku.edu.cn

Objective: Accurately identifying patients achieving pathological complete response (pCR) after neoadjuvant chemoradiotherapy (nCRT) for locally advanced rectal cancer (LARC) not only ensures treatment efficacy but also helps avoid surgical risks. We developed a comprehensive multi-omics model to predict pCR before surgery.

Methods: Clinical data, CT, MRI-T1WI and MRI-T2WI, and radiotherapy dose were collected from 183 LARC patients who underwent preoperative nCRT. Backward stepwise selection, logistic regression, and five-fold cross-validation were employed for the development and validation of a non-imaging model, three radiomics-based models and a dosiomics-based model. These were integrated into a final model, and its performance was tested on multi-center sets.

Results: C_model, based on clinical characteristics, achieved an AUC of 0.85 in the validation set. Radiomics models (CT_model, T1_model, T2_model) exhibited AUCs of 0.66, 0.67, and 0.64, respectively. Dosiomics-based model, D_model, achieved an AUC of 0.75 in validation. The mean AUCs for F_model in the training sets, validation sets, internal and external test sets were 0.90, 0.88, 0.77, and 0.74, respectively.

Conclusion: To assess the efficacy of nCRT in LARC patients, it is crucial to consider clinical characteristics, followed by dosiomics. While T1_model, T2_model and CT_model demonstrate relatively comparable performance, each contributes unique value to the final prediction model.

Keywords: radiomics, dosiomics, nCRT, rectal cancer, predict therapy response

Introduction

Globally, the third most frequently diagnosed cancer is colorectal cancer, of which approximately 30%–50% are rectal cancer cases.[1,2] Rectal cancer accounts for 3.4% of all global cancer-related deaths.[3] Every year, over 700,000 new rectal cancer cases are identified worldwide, with locally advanced rectal cancers (LARC) representing at least 30% of all cases.[3,4] Currently, the standard treatment for LARC is neoadjuvant (chemo) radiotherapy (nCRT) combined with total mesorectal excision (TME).[5–7] The response of LARC to neoadjuvant chemoradiotherapy varies widely among patients, ranging from no tumor regression to achieving pathologic complete response (pCR).[8] Approximately 15–27% of patients exhibit pCR, which has been demonstrated to be a favorable prognostic marker.[9] Although the necessity of surgery in LARC patients with pCR is a subject of ongoing argument, in fact, most patients are still undergoing surgery. Considering surgical complications, especially the complications after nCRT, and the outstanding long-term outcomes in pCR patients apart from surgery, Habr-Gama et al first proposed the "watch-and-wait" approach.[10] The NCCN guidelines have also introduced the "watch-and-wait" nonoperative management strategy,[11] which is applicable to patients who achieve clinical complete response 6–12 weeks after nCRT based on strict clinical evaluation. For these patients, a nonoperative treatment strategy with close follow-up is adopted to monitor the condition of the rectal lesions. Predicting patients who achieve pCR after nCRT can assist doctors in formulating personalized treatment strategies. This

Received: 11 February 2025
Accepted: 14 July 2025
Published: 5 August 2025

helps determine whether patients require surgery or if the "watch-and-wait" approach can be adopted. Therefore, the identification of preoperative pCR gains more and more attention in treatment management.

To predict the treatment response of LARC, clinical analyses have been conducted on the impact of neoadjuvant-intensified chemoradiotherapy in improving overall survival (OS) and disease-free survival (DFS) in LARC patients.[12] The role of oxaliplatin (OXP) in enhancing clinical outcomes has also been studied.[13] Additionally, previous studies have developed a non-imaging clinical risk model to predict treatment response to nCRT with the area under the curve (AUC) about 0.6–0.70.[14–16] With advances in imaging techniques like computed tomography (CT), magnetic resonance imaging (MRI), and functional imaging, there is a growing interest in using visual imaging to accurately detect tumor response to therapy.[17,18] However, visually detecting pCR remains challenging in clinical practice. Radiomics, which extracts high-dimensional data from digital images and reveals non-visual information associated with tumor heterogeneity and pathophysiology, has shown promise in improving pCR prediction models.[19,20] Radiomics-based models have demonstrated an AUC of about 0.8 or higher.[21,22] The development of radiomics has shown great potential in the guidance of cancer treatment and tumor prognosis.[23,24]

According to the research, different prediction outcomes are evident in models constructed using various image modalities.[25–29] Magnetic resonance imaging is considered the most recommended and promising method among all modalities owing to its high soft tissue resolution, functional and quantitative imaging capabilities, and non-ionizing radiation. MRI is the preferred method for local staging of rectal cancer, and it also has a wide range of clinical application in the prognosis assessment. Studies have found that DW-MRI can provide functional imaging information about tissue cellular density and water molecule diffusion, showing potential in assessing the response to neoadjuvant therapy.[30] MRI-related radiomics have also been applied in certain prediction models to assess tumor response to nCRT in LARC. Some studies focused solely on MRI images acquired before nCRT, which may have inherent limitations in reflecting the impact of nCRT on the target population, as a single imaging modality cannot comprehensively capture the tumor's condition. Other studies have examined the differences between pre-nCRT and post-nCRT MRI scans (delta radiomics, Δradiomics) for tumor response prediction, leading to improved pCR prediction.[22,31] However, these studies still relied on a single imaging modality and did not fully exploit the potential of multimodal data.

Furthermore, target dose plays a crucial role in determining the effectiveness of treatment, and clinical dosimetric parameters are essential in predicting the response to treatment.[32,33] By understanding and optimizing the target dose through these parameters, medical professionals can improve treatment outcomes and provide more personalized care for patients. In theory, modeling based on the mentioned clinical non-imaging parameters, imaging parameters, and dosimetric parameters would lead to a more comprehensive and accurate prediction of whether preoperative LARC patients who underwent neoadjuvant chemoradiotherapy have reached the pCR level. However, due to various reasons such as data collection limitations, severe data missing and complex data preprocessing, existing studies have mostly focused on building non-imaging models based on clinical characteristics,[14–16] single-modality imaging models,[17,18] single dosimetric models,[34,35] or combinations of two of these models.[21,36] Moreover, these studies are limited to their own research center's data and lack external validation datasets to test the generalizability of the models.

To address the limitations of existing models and considering the high incidence of LARC as well as the need for personalized treatment, this study introduces an innovative approach by integrating multi-omics data to develop and validate a comprehensive pCR prediction model. This model not only incorporates clinical features but also includes radiomic features extracted from pre-nCRT CT and MRI images, as well as dosiomic features derived from dose distribution maps, aiming to enhance predictive accuracy and generalizability. Furthermore, we will validate the model on both internal and external datasets to assess its robustness and clinical applicability, thereby providing more scientific decision support for the precision treatment of LARC patients.

Methods

The research followed the principles outlined in the Declaration of Helsinki and obtained approval from the Ethics Committee of the Peking University Beijing Cancer Hospital and Institute (2018KT78). The Ethics Committee has waived the requirement for patient informed consent; to ensure the protection of participants' privacy, all data have been anonymized. In this study, clinical characteristics, radiomic signatures and dosiomic features were collected from LARC patients, which were divided into a training set and a test set. Five-fold cross-validation was applied. Firstly, data preprocessing was performed to

obtain the optimal subset. Then, the Logistic regression method was used to predict pCR after neoadjuvant chemoradiotherapy. Finally, an external test set was collected to assess the generalization of the model. The specific details are as follows.

Patient Selection

A total of 183 patients with rectal cancer who received nCRT at Beijing Cancer Hospital from January 2019 to December 2022 were retrospectively recruited for modeling training. To be eligible for inclusion, patients had to meet the following criteria: (1) histologically confirmed rectal adenocarcinoma prior to treatment; (2) clinical stage of T3-T4 or any stage T and N+ tumors without distant metastasis according to the 7th edition of the American Joint Committee on Cancer (AJCC); (3) pathological assessment after treatment with TME showing complete pathological response (pCR) defined as T0N0; (4) availability of complete medical records including clinical characteristics, pre-treatment CT, pre-treatment MRI, and dose map. Exclusion criteria included (1) incomplete clinical stage or missing postoperative pathology; (2) poor-quality or incomplete imaging data; (3) incomplete neoadjuvant (chemo)radiotherapy, history of pelvic radiation, double primary cancer, and other factors.

In order to evaluate the generalizability of the model, we collected data from 20 patients with LARC at our institution (BZ test set) and 26 LARC patients from Guowen Hospital (GW test set). The internal test set of 20 patients included complete clinical information, CT, MRI and dose map, and 8 of them achieved pathologically complete responses. A total of 26 patients from Guowen Hospital were selected as the external test set, which includes incomplete clinical features, CT images, dose maps, and 22 cases of diagnostic MRI images.

Data Acquisition

Clinical characteristics included age, gender, pre- and post-treatment levels of carcinoembryonic antigen (CEA), histologic grade, chemotherapy regimens, radiotherapy dose, treatment machine and pre- and post-MRI diagnoses information such as the proportion of tumors invading the entire intestinal wall, maximum thickness, distance outside intestinal wall invasion, cumulative length, distance from the lower edge of the tumor to ARJ, distance from distal tumor margin to anal edge, extramural venous invasion (EMVI) and mesorectal fascia (MRF).

The CT images of internal dataset and external dataset were acquired using Siemens CT scanner (Sensation Open, Siemens, Erlangen, Germany) and Philips CT scanner (Brilliance Big Bore, Philips, Netherlands), respectively. The acquisition parameters are as follows: matrix = 512x512, thickness = 5 mm, kVp = 120 kV. All the MRI scans were performed on a 3.0T scanner (Skyra, Siemens, Erlangen, Germany). Patients underwent contrasted-enhanced T1-weighted and T2-weighted MRI scans using StarVIBE and TSE sequences, respectively. Typical acquisition parameters are as follows: T1WI: TR = 2.83 ms, TE = 1.48 ms, FOV = 380 mm, slice thickness = 3 mm, matrix = 320×320; T2WI: TR = 5770 ms, TE = 96 ms, FOV = 400 mm, slice thickness = 4 mm, matrix = 640×640.

Tumor Segmentation

The entire tumor volume was covered by the gross target volume (GTV), which was drawn manually by radiation oncologists with at least 5 years of experience in rectal cancer radiotherapy. The GTV was subsequently verified by a radiation oncologist with at least 20 years of experience in rectal cancer radiotherapy. To create the planning gross target volume (PGTV), a margin of 0.5 cm was added to the GTV. The PGTV was utilized as the region of interest (ROI), and the CT image structures were deformed onto the registered MRI images.

Feature Extraction

All features were extracted from the ROI using PyRadiomics, which is an open-source platform. We calculated a set of 609 radiomics features, including 37 diagnostics, 14 shape descriptors, 18 first-order statistics, 75 original texture features and 465 Laplacian of Gaussian (LoG) filtered features. Shape descriptors represented the 3-dimensional shape and size of ROI. First-order statistical descriptors, which described the distribution of voxel intensities through commonly used metrics, were directly derived from the image intensity. Texture features were high-order features calculated using the Gray Level Co-occurrence Matrix (GLCM), Gray Level Run Length Matrix (GLRLM), Gray Level Size Zone Matrix (GLSZM), Gray Level Dependence Matrix

(GLDM) and Neighbouring Gray Tone Difference Matrix (NTGDM). The LoG filtered features included first-order statistics and texture classes which were calculated from LoG filtered images.

Feature Selection

The effective features are selected in advance by *T*-test and non-parametric test, and then the optimal subset is obtained by backward stepwise selection (BSS). After *T*-test and non-parametric test, it is assumed that the effective feature number is n, and the corresponding model is M_n. If one feature is removed, the number of features is n-*1* and the model is M_{n-1}. If M_{n-1} model is superior to M_n, the feature is removed, and if not, the feature is retained until all features are traversed.

We used the principal component analysis (PCA) method which is a multivariate statistical technique commonly applied to systematically reduce the number of dimensions needed to describe radiomics features through a decomposition process that filters feature from the largest to smallest spatial scales.

Development and Evaluation of Models

Based on the results of our preliminary experiments, we finally chose the Logistic regression to build the prediction models, including a clinical features-based model (C_model), three radiomics-based models (CT_model, T1_model and T2_model) and a dosiomics-based model (D_model). These five models were integrated into the final model, which is named F_model, representing the multi-omics model. Study workflow and model building are detailed in Figure 1.

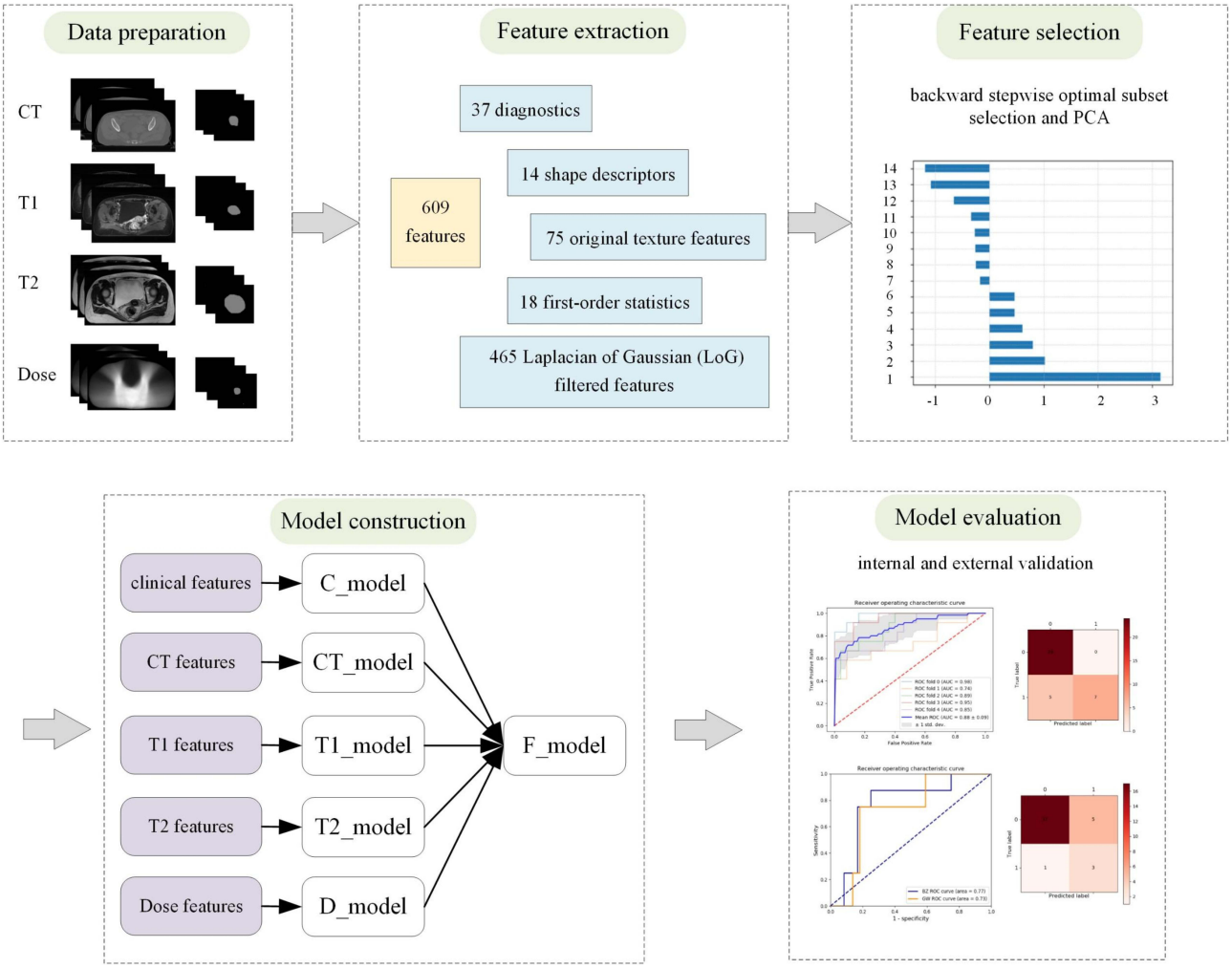

Figure 1 Study workflow and model building. A clinical features-based model (C_model), three radiomics-based models (CT_model, T1_model and T2_model) and a dosiomics-based model (D_model) were integrated into the final model and its performance was verified.

The 183 patients were randomly divided into five equal size subgroups because five-fold cross-validation was applied. Each subgroup was regarded as a validation set and the remaining four-fifths of the patients as the training set. This process was repeated five times with different subgroups to form five training sets and five corresponding validation sets. Evaluation of the above models included discrimination and clinical usefulness. Discrimination performance was quantified based on the AUC of the receiver operating characteristic (ROC) curve. Classification accuracy (ACC) and confusion matrix were also calculated to quantify the discrimination ability of the prediction models.

Results

Patient Characteristics

Patients were divided into pCR group (T0N0, n = 60) and "non-pCR group" (T 1–4, n = 123). Clinical characteristics of the two groups are shown in Table 1. Post-treatment levels of CEA, radiotherapy dose, pre-/post-treatment proportion of tumors invading the entire intestinal wall, distance outside intestinal wall invasion, cumulative length and distance from the lower edge of the tumor to ARJ, and post-treatment maximum thickness are significantly different between the two groups. Clinical characteristics of internal and external test sets in the two groups are detailed in Table 2.

Table 1 Clinical Characteristics of Training and Validation Sets in pCR and Non-pCR Groups

Clinical Characteristic	pCR (n = 60)	Non-pCR (n = 123)	*p*
Age, mean±SD, years	57.02±10.27	58.21±10.00	0.241
Sex (%)			0.255
Male	39 (65)	90 (73.17)	
Female	21 (35)	33 (26.83)	
Pre-treatment levels of CEA, mean±SD	6.44±10.05	7.44±11.22	0.394
Post-treatment levels of CEA, mean±SD	2.88±2.76	4.31±4.69	**0.009**
Histologic grade (%)			0.469
Well differentiated adenocarcinoma	4 (6.67)	4 (3.25)	
Moderately differentiated adenocarcinoma	53 (88.33)	115 (93.5)	
Poorly differentiated adenocarcinoma	3 (5)	4 (3.25)	
Chemotherapy regimens (%)			0.22
Capecitabine	36 (60)	85 (69.11)	
XELOX	24 (40)	38 (30.89)	
Radiotherapy dose (%)			**<0.001**
4180&5060cGy/22f	31 (51.67)	20 (16.26)	
4500&5000cGy/25f	29 (48.33)	103 (83.74)	
Treatment machine (%)			0.126
Varian IX series	47 (78.33)	100 (81.3)	
Varian RAPIDARC	11 (18.33)	23 (18.7)	
Varian TrueBeam series	2 (3.34)	0 (0)	
Pre-/post-treatment MRI diagnoses information			
The proportion of tumors invading the entire intestinal wall, mean±SD	68.86±13.10/ 51.18±15.91	76.24±10.79/ 76.24±10.79	**<0.001**/ **<0.001**
Maximum thickness, mean±SD	17.06±6.10/ 10.68±6.12	16.75±7.64/ 8.98±2.80	0.994/ **<0.001**
Distance outside intestinal wall invasion, mean±SD	3.34±2.22/ 2.42±1.07	5.96±2.51/ 3.54±0.80	**<0.001**/ **<0.001**
Cumulative length, mean±SD	46.56±12.53/ 29.21±6.61	48.82±9.34/ 34.91±6.48	**<0.001**/ **<0.001**
Distance from the lower edge of the tumor to ARJ, mean±SD	19.13±11.28/ 23.95±10.51	28.93±18.42/ 35.76±16.06	**<0.001**/ **<0.001**
Distance from distal tumor margin to anal edge, mean±SD	44.67±28.94/ 51.55±33.77	47.04±23.78/ 50.37±25.47	0.86/ 0.40

(*Continued*)

Table 1 (Continued).

Clinical Characteristic	pCR (n = 60)	Non-pCR (n = 123)	*p*
EMVI	2.15±1.44/ 1.50±1.20	3.44±6.80/ 2.23±1.14	**0.009**/ **0.009**
MRF			0.881/ 0.991
0	29 (48.33)/ 22 (36.67)	58 (47.15)/ 45 (36.59)	
1	31 (51.67)/ 38 (63.33)	65 (52.85)/ 78 (63.41)	

Notes: The bold font indicates that there are significant differences in the corresponding clinical characteristics between the pCR and non-pCR groups.
Abbreviations: SD, standard deviation; CEA, carcinoembryonic antigen; n, number of patients in the corresponding group; (%), The numbers in parentheses represent the percentage of the total; f, frequency, 22f, 22 sessions of radiotherapy have been performed.

Table 2 Clinical Characteristics of Test Sets in pCR and Non-pCR Groups

Clinical Characteristic	Internal Test (n = 20)		External Test (n = 26)	
	pCR (n = 8)	Non-pCR (n = 12)	pCR (n = 4)	Non-pCR (n = 22)
Age, mean±SD, years	59.25±9.57	59.33±6.68	58.50±4.80	60.23±8.65
Sex (%)				
Male	7 (87.5)	10 (83.33)	3 (75)	13 (59.09)
Female	1 (12.5)	2 (16.67)	1 (25)	9 (40.91)
Pre-treatment levels of CEA, mean±SD	4.20±1.33	3.28±1.58	4.92±6.03	3.72±5.12
Post-treatment levels of CEA, mean±SD	1.60±0.78	3.06±1.06	2.36±1.46	2.08±1.40
Histologic grade (%)				
Well differentiated adenocarcinoma	2 (25)	2 (16.67)	0 (0)	0 (0)
Moderately differentiated adenocarcinoma	4 (50)	9 (75)	4 (100)	21 (95.45)
Poorly differentiated adenocarcinoma	2 (25)	1 (8.33)	0 (0)	1 (4.55)
Chemotherapy regimens (%)				
Capecitabine	6 (75)	7 (58.33)	–	–
XELOX	2 (25)	5 (41.67)	–	–
Radiotherapy dose (%)				
4180&5060cGy/22f	8 (100)	9 (16.26)	0 (0)	0 (0)
4500&5000cGy/25f	0 (0)	3 (83.74)	4 (100)	22 (100)
Treatment machine (%)				
Varian IX series	8 (100)	12 (100)	–	–
Varian RAPIDARC	0 (0)	0 (0)	–	–
Varian TrueBeam series	0 (0)	0 (0)	–	–

Abbreviations: SD, standard deviation; CEA, carcinoembryonic antigen; n, number of patients in the corresponding group; (%), The numbers in parentheses represent the percentage of the total; f, frequency, 22f, 22 sessions of radiotherapy have been performed.

Selection of Features

After feature pre-screening, the C model, CT_model, T1_model, T2_model and D_model had 7, 10, 7, 11 and 6 features, respectively. Subsequently, the optimal subset was obtained using BBS, resulting in 6, 9, 6, 6 and 4 features for the respective models. In the end, 14 features were selected for constructing the F_model: 6 clinical characteristics, 2 dosiomic features and 6 radiomic signatures, the details were shown in Figure 2.

Results of the Training and Validation Sets

The ACC and AUC of training and validation sets in C_model, CT_model, T1_model, T2_model, D_model and F_model was detailed Table 3, and the ROC curve of the corresponding five-fold cross-validation was shown in Figure 3. When considering the

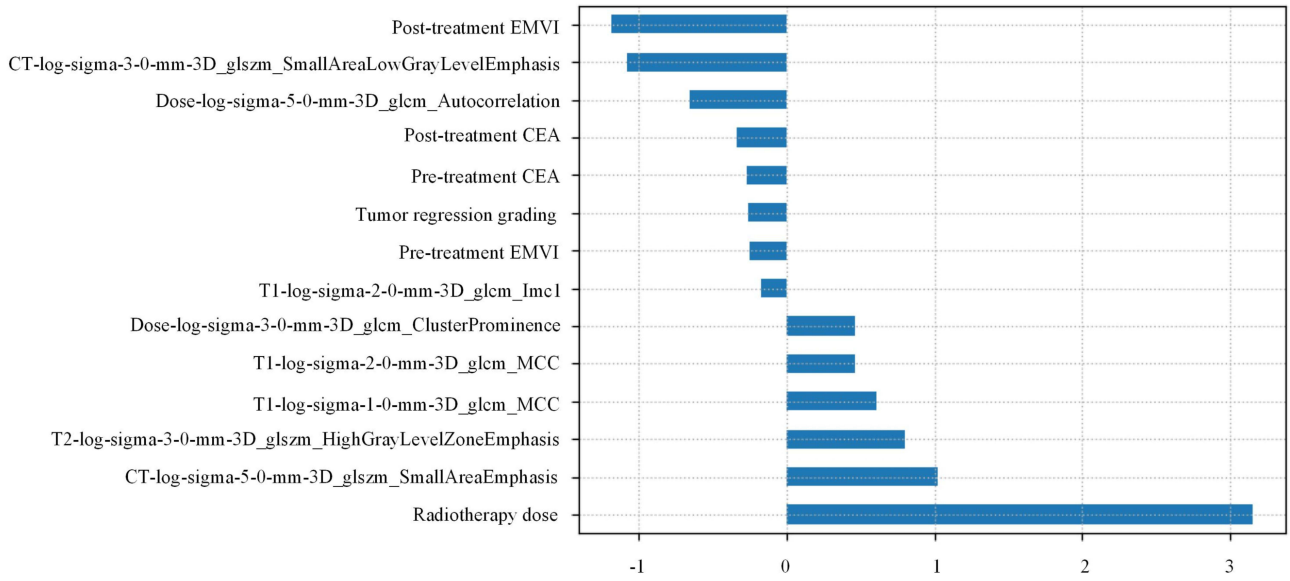

Figure 2 Feature contributions of F_model.

C_model generated from the selected clinical characteristics alone, the mean AUC of 0.86 (standard deviation [SD] 0.02) in the training set and 0.85 (SD 0.10) in the validation set (Figure 3a) were obtained. Additionally, the mean ACCs were 0.84 (SD 0.01) and 0.83 (SD 0.06) for the training and validation sets, respectively. Similarly, when considering the CT_model generated solely from CT radiomics, the mean AUC was 0.68 (SD 0.02) for the training set and 0.66 (SD 0.10) for the validation set (Figure 3b). The mean ACCs for the training and validation sets were 0.67 (SD 0.02) and 0.66 (SD 0.04), respectively. The AUCs the T1_model and T2_model, generated solely from T1 radiomics and T2 radiomics respectively, were comparable to the CT_model. The dosiomic based model, D_model, demonstrated a satisfactory discrimination, with mean AUCs of 0.77 (SD 0.03) and 0.75 (SD 0.11) in the training and validation sets (Figure 3e), respectively.

The clinical characteristics combined with radiomics and dosiomics generated the F_model, which clearly outperformed the single-modality clinical based model and radiomic based model. In the training and validation sets, the mean ACCs were 0.86 (SD 0.02) and 0.85 (SD 0.06), respectively. Furthermore, the mean AUC was 0.90 (SD 0.02) for the training set and 0.88 (SD 0.09) for the validation set (Figure 3f). The confusion matrixes of the validation set for the six mentioned models were presented in Figure 4.

Results of the Internal and External Test Sets

The accuracy scores for the C_model, CT_model, T1_model, T2_model, D_model and F_model in the internal test set were 0.80, 0.65, 0.70, 0.65, 0.70 and 0.75, respectively. The AUCs were 0.73, 0.64, 0.62, 0.64, 0.71 and 0.77, respectively. In the external test set, the C_model achieved an accuracy score of 0.65 and an AUC of 0.67. The CT_model scored 0.81 in ACC and 0.65 in AUC. In T1_model and T2_model, the ACC and AUC were 0.77 and 0.62, 0.82 and 0.67, respectively. The ACC and AUC of D_model was 0.81 and 0.74, respectively. The F_model scored 0.77 in ACC and 0.74 in AUC. The details of test results for internal and external test sets were listed in Table 4. The ROC curves of the internal and external test sets for the different models were displayed in Figure 5.

Table 3 ACC and AUC Results for Training and Validation Sets of Different Models

		C_model	CT_model	T1_model	T2_model	D_model	F_model
ACC	Train	0.84±0.01	0.67±0.02	0.74±0.02	0.70±0.02	0.76±0.02	0.86±0.02
	Validation	0.83±0.06	0.66±0.04	0.74±0.05	0.69±0.03	0.73±0.10	0.85±0.06
AUC	Train	0.86±0.02	0.68±0.02	0.67±0.02	0.63±0.02	0.77±0.03	0.90±0.02
	Validation	0.85±0.10	0.66±0.10	0.67±0.09	0.64±0.08	0.75±0.11	0.88±0.09

https://doi.org/10.2147/CMAR.S517949

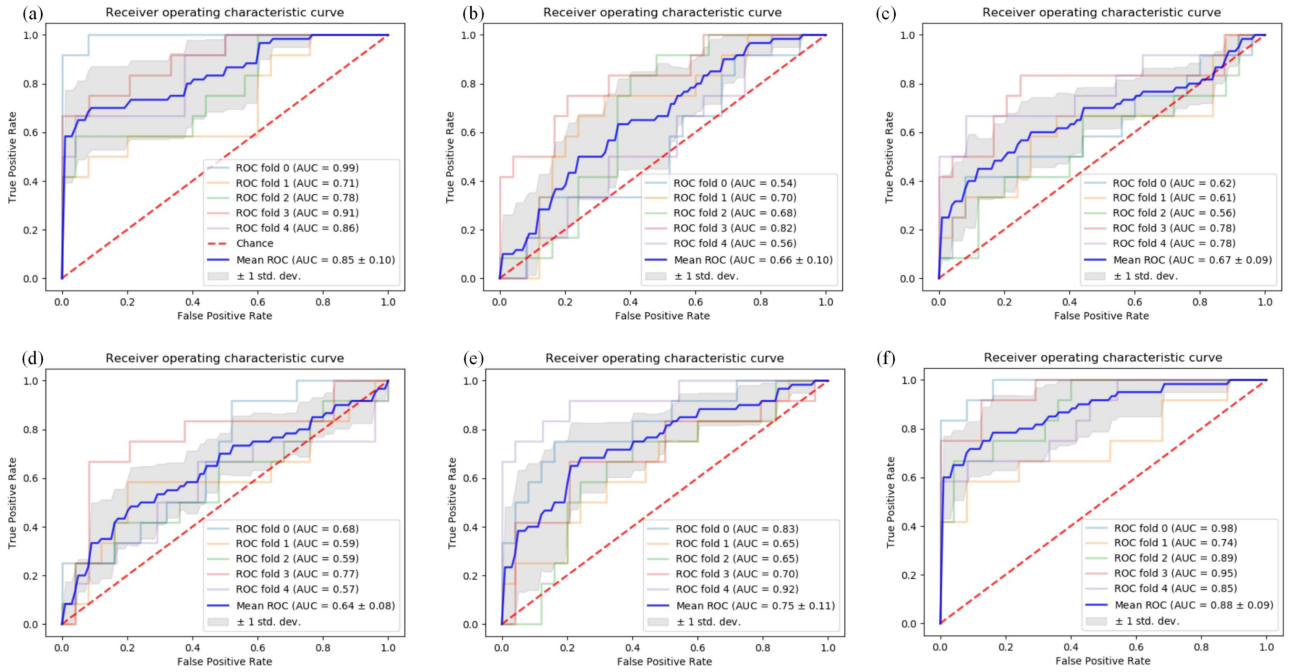

Figure 3 ROC curves for C_model, CT_model, T1_model, T2_model, D_model and F_model. (**a**) ROC curve for the C_model in the validation set, showing a mean AUC of 0.85 (SD 0.10). (**b**) ROC curve for the CT_model in the validation set, showing a mean AUC of 0.66 (SD 0.10). (**c**) ROC curve for the T1_model in the validation set, showing a mean AUC of 0.67 (SD 0.09). (**d**) ROC curve for the T2_model in the validation set, showing a mean AUC of 0.64 (SD 0.08). (**e**) ROC curve for the D_model in the validation set, showing a mean AUC of 0.75 (SD 0.11). (**f**) ROC curve for the F_model in the validation set, showing a mean AUC of 0.88 (SD 0.09). Receiver-operating characteristic, ROC; clinical characteristics, C_model; CT-based radiomics, CT_model; T1WI-based radiomics, T1_model; T2WI-based radiomics, T2_model; Dose-based dosiomics, D_model; clinical characteristics combined with radiomics and dosiomics, F_model.

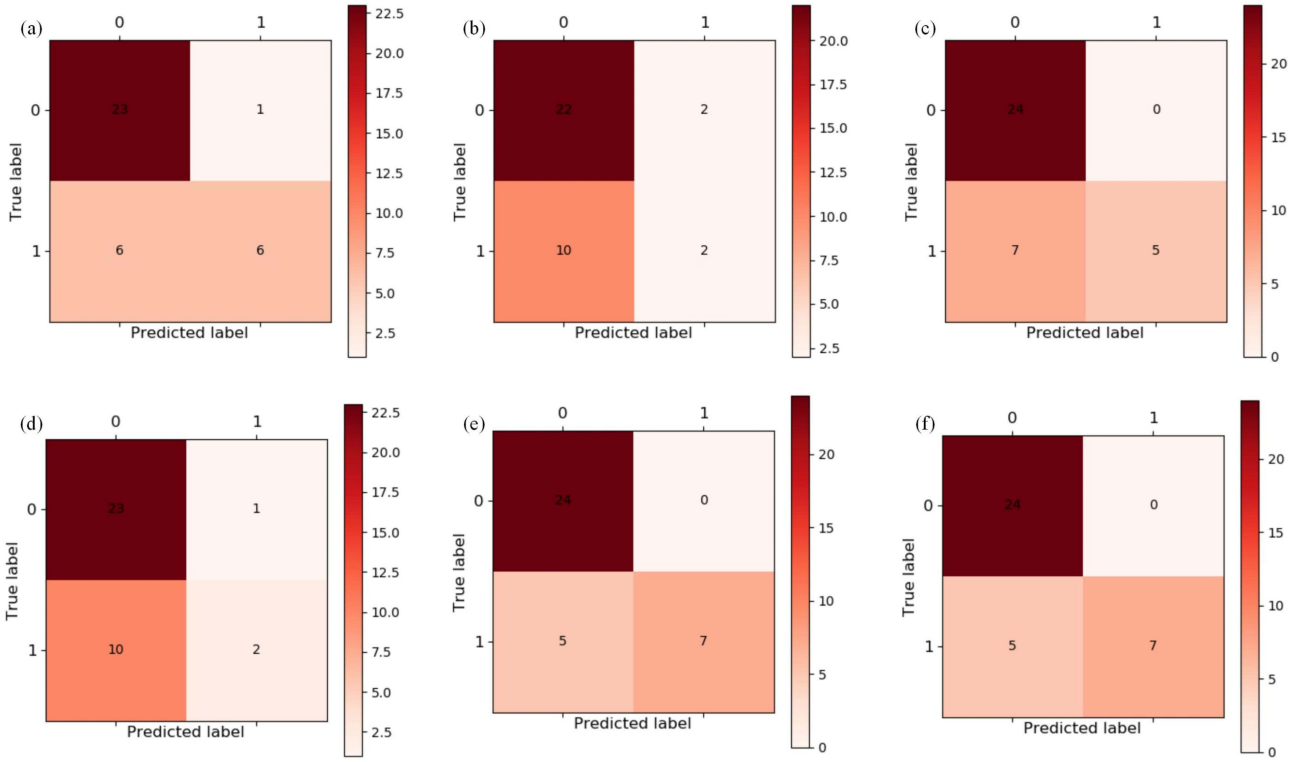

Figure 4 The confusion matrixes of the C_model (**a**), CT_model (**b**), T1_model (**c**), T2_model (**d**), D_model (**e**) and F_model (**f**).

Table 4 ACC and AUC Results for Internal and External Test Sets of Different Models

		C_model	CT_model	T1_model	T2_model	D_model	F_model
BZ test	ACC	0.80	0.65	0.70	0.65	0.70	0.75
	AUC	0.73	0.64	0.62	0.64	0.71	0.77
GW test	ACC	0.65	0.81	0.77	0.82	0.81	0.77
	AUC	0.67	0.65	0.62	0.67	0.74	0.74

The confusion matrix of the internal and external test sets for the C_model, CT_model, T1_model, T2_model, D_model and F_model was presented in Figure 6. C_model demonstrates favorable performance on the internal test set, but exhibits limited capability to differentiate true positive cases on the external test set. Both the radiomic-based model

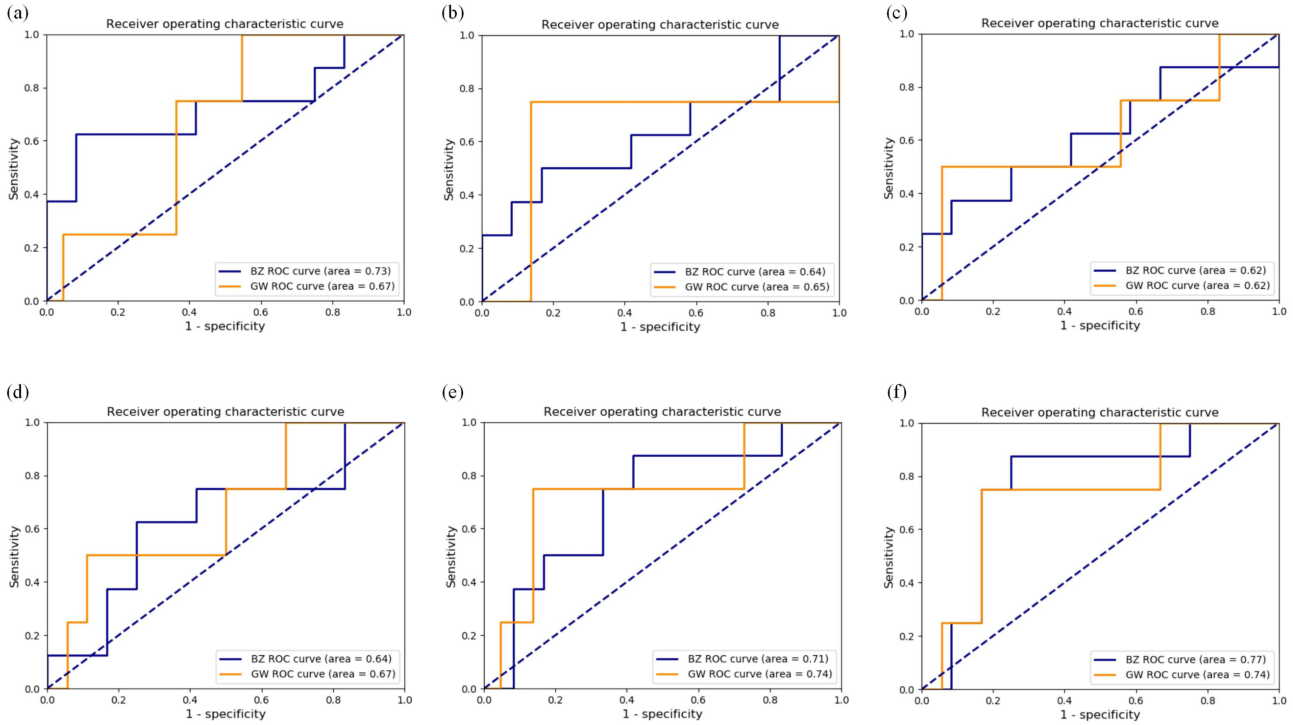

Figure 5 ROC curves of the internal and external test sets for C_model, CT_model, T1_model, T2_model, D_model and F_model. The solid blue line represents the internal test results and the Orange is the external test results. (**a**) Testing with C_model; (**b**) Testing with CT_model; (**c**) Testing with T1_model; (**d**) Testing with T2_model; (**e**) Testing with D_model; (**f**) Testing with F_model.

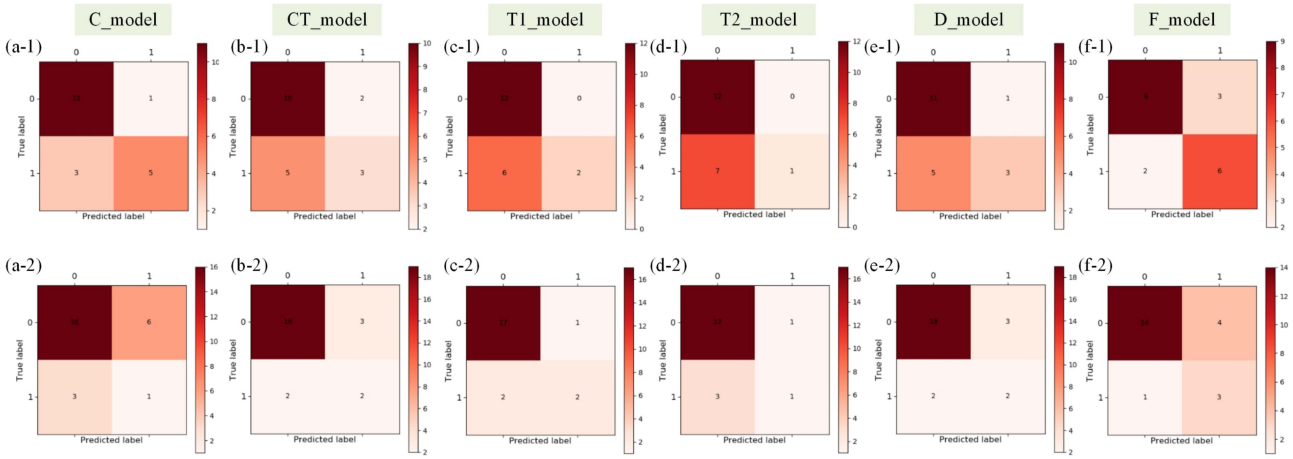

Figure 6 The confusion matrixes of the internal test set and external test set. (**a–f**) represents the results of tests using C_model, CT_model, T1_model, T2_model, D_model and F_model, respectively. (−1) and (−2) indicate internal and external test, respectively.

https://doi.org/10.2147/CMAR.S517949

and the dosiomic-based model demonstrate strong ability to distinguish true negative cases, while they have limitations in accurately distinguishing true positive cases. F_model exhibits excellent ability to judge both true positive and true negative cases on both the internal and external test sets.

Discussion

There are various factors affecting the pathologic response to nCRT in LARC. In this study, we generated a multi-omics model by synthesizing clinical characteristics, radiomic and dosiomic features. The generalization performance of the model was tested with internal and external test sets. Single-modality prediction models based on clinical characteristics, radiomic and dosiomic features were also established and validated. The multi-omics model clearly outperformed the single-modality clinical-based model, single radiomic-based model and single dosiomic-based model. The dosiomic-based model outperformed the radiomics based models. While the radiomics based models (including T1_model, T2_model and CT_model) had relatively similar performance, each contributed a certain value to the final prediction model. The multi-omics model achieved an accuracy and AUC of approximately 0.75 in both the internal and external test sets. Additionally, our data revealed that post-treatment CEA levels, the total radiation dose, the frequency of radiotherapy were associated with pCR, which was in accordance with the results of previous studies.[15,37–40]

In previous clinical prediction models, there has little consideration for the diagnostic information from MRI before and after treatment. This study showed that pre-/post-treatment proportion of tumors invading the entire intestinal wall, distance outside intestinal wall invasion, cumulative length and distance from the lower edge of the tumor to ARJ, and post-treatment maximum thickness were significantly different between the pCR group and non-pCR group. Therefore, it showed significantly better discrimination based on clinical characteristics alone. The post-treatment levels of CEA and radiotherapy dose are also significantly different between the pCR group and non-pCR group. However, after feature pre-screening, the C model had seven features instead of eight. The reason is that although there are significant differences between two groups, the features contribute differently to the model. In order to obtain the optimal subset, we used BSS method to further screen the features. In the end, 14 features were selected for constructing the F_model: 6 clinical characteristics, 2 dosiomic features and 6 radiomic signatures, the details were shown in Figure 2.

The recently established models for predicting tumor response were either based on the single radiomic features, single radiomic signatures, single clinical characteristics, or they were derived from studies conducted on single-center cohorts.[39,41,42] With advancements in technology to minimize variability in acquisition parameters of various cancer centers, multi-center radiomics has been attempted in rectal cancer.[21,43,44] Song et al successfully developed and validated MRI-based multicenter radiomic model to predict treatment response using multi-center data from a considerably large sample of patients, but without external testing. We used small-scale, more comprehensive data to build a multi-omics model that produces better predictive results, and we achieved decent external test results. Due to the lack of certain clinical information and MRI features in the external test set, the external test results were slightly worse than the internal test results. In addition, the phenomenon where the multi-omics model performed exceptionally well on the internal training and validation sets but showed a significant decline in performance during testing, particularly on external test data from different centers, could be due to factors such as overfitting, data sources, scanning conditions, and other factors.

It is a long-term research work to build the prediction model and improve the performance of the model by integrating all the information of the clinical characteristics, radiomic and dosiomic signatures. In this study, there are several limitations. First, the training and validation sets were only collected 183 cases because of the incomplete clinical information of some patients. Expanding the dataset, including the training set, validation set, and test set, may further enhance the impact and applicability of the study. Second, logistic regression was selected to construct the prediction model because it is well-suited to small sample sizes and datasets with a limited number of features, such as radiomics data. Moreover, since the prediction task in this study (eg, pCR prediction) is a binary classification problem, logistic regression offers stable and interpretable performance in this context. Nevertheless, the model requires further optimization through the exploration of other classification algorithms and the application of more standardized engineering strategies. Finally, diagnosis and treatment information such as clinical stages, treatment modalities, DWI, and contrast-

enhanced T1WI was not included in the study, and this information of patients can be further supplemented in the future to build a more accurate prediction model.

Conclusions

We have developed and validated a multi-omics model based on clinical characteristics, pre-treatment radiomic, and dosiomics signatures to predict pCR in patients with LARC. This model can help identify LARC patients who can benefit from organ preservation strategies and avoid overtreatment.

Ethics Approval and Consent to Participate

This multi-centre study was conducted in accordance with the Declaration of Helsinki and was approved by the Ethics Committee of the Peking University Beijing Cancer Hospital and Institute (2018KT78), and the requirement for individual informed patient consent waived owing to the retrospective nature of the study.

Acknowledgments

Thanks to Jingyuan Wang from the Department of Biostatistics at Peking University for providing statistical support and to Zhexiang Song from the Department of Physics at Beihang University for providing the partial code support. The abstract of this work was previously presented at the AOCMP-SEACOMP 2024 conference, held from 10 to 13 October 2024 in Penang, Malaysia. It was published in the *Physical and Engineering Sciences in Medicine* conference proceedings, on pages 4–5 (https://link.springer.com/article/10.1007/s13246-024-01502-0).

Funding

This work was supported in part by the Natural Science Foundation of China(12475309), Beijing Natural Science Foundation (Z210008), the Natural Science Foundation of China (82371112, 62394311, 62394310, 12275012, 12411530076, 82202941), Foundation of Peking University Cancer Hospital (PY202305), Fundamental Research Funds for the Central Universities/Clinical Medicine Plus X - Young Scholars Project of Peking University (PKU2025PKULCXQ014); Ministry of Education Exchange Program for Teachers and Students of Higher Education Institutions in the Chinese Mainland/Hong Kong/Macao (7111400072); Inner Mongolia Science & Technology Project Plan (2022YFSH0064) and Clinical scientist training program of Peking University (BMU2023PYJH009 to Ping Jiang).

Disclosure

The authors report no conflicts of interest in this work.

References

1. Bray F, Ferlay J, Soerjomataram I, et al. Global cancer statistics 2018: GLOBOCAN estimates of incidence and mortality worldwide for 36 cancers in 185 countries. *CA Cancer J Clin*. 2018;68(6):394-424. doi:10.3322/caac.21492
2. Bailey CE, Hu CY, You YN, et al. Increasing disparities in the age- related incidences of colon and rectal cancers in the United States. *JAMA Surg*. 2015;150(1):17-22. doi:10.1001/jamasurg.2014.1756
3. Hyuna S, Jacques F, Rebecca LS, et al. Global cancer statistics 2020: GLOBOCAN estimates of incidence and mortality worldwide for 36 cancers in 185 countries. *CA Cancer J Clin*. 2021;71(3):209–249. doi:10.3322/caac.21660
4. Siegel RL, Miller KD, Fedewa SA, et al. Colorectal cancer statistics, 2017. *CA Cancer J Clin*. 2017;67(3):177–193. doi:10.3322/caac.21395
5. Naohiro T, Hideyuki I, Kohji T, et al. Japanese society for cancer of the colon and rectum (JSCCR) guidelines 2020 for the clinical practice of hereditary colorectal cancer. *Int J Clin Oncol*. 2021;26(8):1353-1419. doi:10.1007/s10147-021-01881-4
6. Glynne-Jones R, Wyrwicz L, Tiret E, et al. Rectal cancer: ESMO clinical practice guidelines for diagnosis, treatment and follow-up. *Ann Oncol*. 2017;28(suppl_4):iv22–iv40. doi:10.1093/annonc/mdx224
7. Benson AB, Venook AP, Al-Hawary MM, et al. NCCN guidelines insights: rectal cancer, version 6.2020. *J Natl Compr Canc Netw*. 2020;18 (7):806–815. doi:10.6004/jnccn.2020.0032
8. Smith FM, Winter D. Pathologic complete response of primary tumor following preoperative chemoradiotherapy for locally advanced rectal cancer: long-term outcomes and prognostic significance of pathologic nodal status (KROG 09-01). *Ann Surg*. 2017;265(4):e27–e28. doi:10.1097/SLA.0000000000000462
9. Maas M, Nelemans PJ, Valentini V, et al. Long-term outcome in patients with a pathological complete response after chemoradiation for rectal cancer: a pooled analysis of individual patient data. *Lancet Oncol*. 2010;11(9):835–844. doi:10.1016/S1470-2045(10)70172-8
10. Perez RO. Complete clinical response in rectal cancer: a turning tide. *Lancet Oncol*. 2016;17(2):125-126. doi:10.1016/S1470-2045(15)00487-8

11. Benson AB, Venook AP, Adam M, et al. NCCN guidelines® insights: rectal cancer, version 3.2024. *J Natl Compr Canc Netw*. 2024;22(6):366–375. doi:10.6004/jnccn.2024.0041
12. Musio D, De Felice F, Bulzonetti N, et al. Neoadjuvant-intensified treatment for rectal cancer: time to change? *World J Gastroenterol*. 2013;19(20):3052–3061. doi:10.3748/wjg.v19.i20.3052
13. De Felice F, Benevento I, Magnante AL, et al. Clinical benefit of adding oxaliplatin to standard neoadjuvant chemoradiotherapy in locally advanced rectal cancer: a meta-analysis: oxaliplatin in neoadjuvant treatment for rectal cancer. *BMC Cancer*. 2017;17(1):325. doi:10.1186/s12885-017-3323-4
14. Van Stiphout RG, Lammering G, Buijsen J, et al. Development and external validation of a predictive model for pathological complete response of rectal cancer patients including sequential PET-CT imaging. *Radiother Oncol*. 2011;98(1):126–133. doi:10.1016/j.radonc.2010.12.002
15. Huh JW, Kim HR, Kim YJ. Clinical prediction of pathological complete response after preoperative chemoradiotherapy for rectal cancer. *Dis Colon Rectum*. 2013;56(6):698–703. doi:10.1097/DCR.0b013e3182837e5b
16. Joye I, Debucquoy A, Fieuws S, et al. Can clinical factors be used as a selection tool for an organ-preserving strategy in rectal cancer? *Acta Oncol*. 2016;55(8):1047–1052. doi:10.3109/0284186X.2016.1167954
17. Kim SH, Lee JM, Hong SH, et al. Locally advanced rectal cancer: added value of diffusion-weighted MR imaging in the evaluation of tumor response to neoadjuvant chemo- and radiation therapy. *Radiology*. 2009;253(1):116–125. doi:10.1148/radiol.2532090027
18. Wang JZ, Shen LJ, Zhong HY, et al. Radiomics features on radiotherapy treatment planning CT can predict patient survival in locally advanced rectal cancer patients. *Sci Rep*. 2019;9(1):15346. doi:10.1038/s41598-019-51629-4
19. Gillies RJ, Kinahan PE, Hricak H. Radiomics: images are more than pictures, they are data. *Radiology*. 2016;278(2):563-577. doi:10.1148/radiol.2015151169
20. Kiessling F. The changing face of cancer diagnosis: from computational image analysis to systems biology. *Eur Radiol*. 2018;28(8):3160-3164. doi:10.1007/s00330-018-5347-9
21. Song M, Li S, Wang H, et al. MRI radiomics independent of clinical baseline characteristics and neoadjuvant treatment modalities predicts response to neoadjuvant therapy in rectal cancer. *Br J cancer*. 2022;127(2):249–257. doi:10.1038/s41416-022-01786-7
22. Yuqiang L, Liu W, Pei Q, et al. Predicting pathological complete response by comparing MRI-based radiomics pre- and post-neoadjuvant radiotherapy for locally advanced rectal cancer. *Cancer Med*. 2019;8(17):7244–7252. doi:10.1002/cam4.2636
23. Horvat N, Bates DDB, Petkovska I. Novel imaging techniques of rectal cancer: what do radiomics and radiogenomics have to offer? A literature review. *Abdom Radio*. 2019;44(11):3764–3774. doi:10.1007/s00261-019-02042-y
24. Mahadevan LS, Zhong J, Venkatesulu B, et al. Imaging predictors of treatment outcomes in rectal cancer: an overview. *Crit Rev Oncol Hematol*. 2018;129:153–162. doi:10.1016/j.critrevonc.2018.06.009
25. van Stiphout RG, Valentini V, Buijsen J, et al. Nomogram predicting response after chemoradiotherapy in rectal cancer using sequential PETCT imaging: a multicentric prospective study with external validation. *Radiother Oncol*. 2014;113(2):215-222. doi:10.1016/j.radonc.2014.11.002
26. Gollub MJ, Tong T, Weiser M, Zheng J, Gonen M, Zakian KL. Limited accuracy of DCE-MRI in identification of pathological complete responders after chemoradiotherapy treatment for rectal cancer. *Eur Radiol*. 2017;27(4):1605-1612. doi:10.1007/s00330-016-4493-1
27. Sun YS, Zhang XP, Tang L, et al. Locally advanced rectal carcinoma treated with preoperative chemotherapy and radiation therapy: preliminary analysis of diffusion-weighted MR imaging for early detection of tumor histopathologic downstaging. *Radiology*. 2010;254(1):170-178. doi:10.1148/radiol.2541082230
28. Yu J, Xu Q, Song JC, et al. The value of diffusion kurtosis magnetic resonance imaging for assessing treatment response of neoadjuvant chemoradiotherapy in locally advanced rectal cancer. *Eur Radiol*. 2017;27(5):1848-1857. doi:10.1007/s00330-016-4529-6
29. Nougaret S, Vargas HA, Lakhman Y, et al. Intravoxel incoherent motion-derived histogram metrics for assessment of response after combined chemotherapy and radiation therapy in rectal cancer: initial experience and comparison between single-section and volumetric analyses. *Radiology*. 2016;280(2):446-454. doi:10.1148/radiol.2016150702
30. Musio D, De Felice F, Magnante AL, et al. Diffusion-weighted magnetic resonance application in response prediction before, during, and after neoadjuvant radiochemotherapy in primary rectal cancer carcinoma. *Biomed Res Int*. 2013;2013:740195. doi:10.1155/2013/740195
31. Peeken JC, Asadpour R, Specht K, et al. MRI-based delta-radiomics predicts pathologic complete response in high-grade soft-tissue sarcoma patients treated with neoadjuvant therapy. *Radiother Oncol*. 2021;164:73–82. doi:10.1016/j.radonc.2021.08.023
32. Bhishamjit SC, Carlos V, Christopher GM, et al. Dosimetric study of pelvic proton radiotherapy for high-risk prostate cancer. *Int J Radiat Oncol Biol Phys*. 2009;75(4):994–1002. doi:10.1016/j.ijrobp.2009.01.044
33. Kim KH, Cho BC, Lee CG, et al. Hippocampus-sparing whole-brain radiotherapy and simultaneous integrated boost for multiple brain metastases from lung adenocarcinoma: early response and dosimetric evaluation. *Technol Cancer Res Treat*. 2016;15(1):122–129. doi:10.1177/1533034614566993
34. Yang SS, OuYang PY, Guo JG, et al. Dosiomics risk model for predicting radiation induced temporal lobe injury and guiding individual intensity-modulated radiation therapy. *Int J Radiat Oncol Biol Phys*. 2023;115(5):1291–1300. doi:10.1016/j.ijrobp.2022.11.036
35. Murakami Y, Soyano T, Kozuka T, et al. Dose-based radiomic analysis (dosiomics) for intensity modulated radiation therapy in patients with prostate cancer: correlation between planned dose distribution and biochemical failure. *Int J Radiat Oncol Biol Phys*. 2022;112(1):247–259. doi:10.1016/j.ijrobp.2021.07.1714
36. Kawahara D. Radiomics and dosiomics for predicting complete response to definitive chemoradiotherapy patients with esophageal squamous cell cancer with hybrid institution model. *Int J Radiat Oncol Biol Phys*. 2022;114(3):e99. doi:10.1016/j.ijrobp.2022.07.890
37. Buijsen J, van Stiphout RG, Menheere PP, Lammering G, Lambin P. Blood bio-markers are helpful in the prediction of response to chemoradiation in rectal cancer: a prospective, hypothesis driven study on patients with locally advanced rectal cancer. *Radiother Oncol*. 2014;111(2):237–242. doi:10.1016/j.radonc.2014.03.006
38. Gash KJ, Baser O, Kiran RP. Factors associated with degree of tumour response to neo-adjuvant radiotherapy in rectal cancer and subsequent corresponding outcomes. *Eur J Surg Oncol*. 2017;43(11):2052–2059. doi:10.1016/j.ejso.2017.07.024
39. Appelt AL, Ploen J, Vogelius IR, Bentzen SM, Jakobsen A. Radiation dose-response model for locally advanced rectal cancer after preoperative chemoradiation therapy. *Int J Radiat Oncol Biol Phys*. 2013;85(1):74–80. doi:10.1016/j.ijrobp.2012.05.017
40. Rodel C, Liersch T, Becker H, et al. Preoperative chemoradiotherapy and postoperative chemotherapy with fluorouracil and oxaliplatin versus fluorouracil alone in locally advanced rectal cancer: initial results of the German CAO/ARO/AIO-04 randomised Phase 3 trial. *Lancet Oncol*. 2012;13(7):679–687. doi:10.1016/S1470-2045(12)70187-0

41. Zhou XZ, Yi YJ, Liu ZY, et al. Radiomics-based pretherapeutic prediction of non-response to neoadjuvant therapy in locally advanced rectal cancer. *Ann Surg Oncol*. 2019;26(6):1676–1684. doi:10.1245/s10434-019-07300-3
42. Cui YF, Yang XT, Shi ZQ, et al. Radiomics analysis of multiparametric MRI for prediction of pathological complete response to neoadjuvant chemoradiotherapy in locally advanced rectal cancer. *Eur Radio*. 2019;29(3):1211–1220. doi:10.1007/s00330-018-5683-9
43. van Griethuysen JJM, Lambregts DMJ, Trebeschi S, et al. Radiomics performs comparable to morphologic assessment by expert radiologists for prediction of response to neoadjuvant chemoradiotherapy on baseline staging MRI in rectal cancer. *Abdom Radiol*. 2020;45(3):632–643. doi:10.1007/s00261-019-02321-8
44. Dinapoli N, Barbaro B, Gatta R, et al. Magnetic resonance, vendor-independent, intensity histogram analysis predicting pathologic complete response after radiochemotherapy of rectal cancer. *Int J Radiat Oncol Biol Phys*. 2018;102(4):765–774. doi:10.1016/j.ijrobp.2018.04.065